ISSN 2176-5480

22nd International Congress of Mechanical Engineering (COBEM 2013)
November 3-7, 2013, Ribeirão Preto, SP, Brazil

WSGG MODEL EVALUATION IN A STRONGLY NON-ISOTHERMAL AND INHOMOGENEOUS MEDIUM COMPOSED OF CO_2 AND H_2O

Gustavo Duciak
Rogério Brittes
Fabiano Cassol
Felipe Roman Centeno
Francis H. R. França
Federal University of Rio Grande do Sul, Porto Alegre, RS, Brazil

gustavo@apsengenharia.com.br
rogeriobrittes@mecanica.ufrgs.br
fabiano.cassol@ufrgs.br
frcenteno@mecanica.ufrgs.br
frfranca@mecanica.ufrgs.br

Abstract. *Strongly non-isothermal and non-homogeneous conditions are frequent in combustion problems. In these situations, radiation is the main heat transfer mode and is very difficult to be modeled. Due to the strong dependence of the absorption coefficient on the wavenumber, the adequate prediction of the radiative heat transfer rates demand some spectral modeling. The weighted-sum-of-gray-gases (WSGG) model is an alternative to the line-by-line (LBL) integration, which is computationally expensive. In this work, some temperature and concentrations one-dimensional profiles, obtained from a combustion chamber, are used to represent non-isothermal and non-homogenous medium comprised by carbon dioxide and water vapor. The WSGG results present good concordance with the LBL benchmark solution.*

Keywords: *weighted-sum-of-gray-gases, radiation heat transfer, line-by-line.*

1. INTRODUCTION

Thermal radiation is the main mechanism of heat exchange in combustion process. The spectral integration of the radiative transfer equation (RTE) is still a difficult task due to the highly irregular dependence of the absorption coefficient on the wavenumber. The line-by-line (LBL) integration, known as benchmark solution, is computationally expensive due to many thousands of absorption lines that exist in the spectra of gases. To overcome this drawback there are the global models, which are alternatives to spectral integration of the RTE.

The weighted-sum-of-gray-gases (WSGG) model, introduced by Hottel and Sarofim (1967) in the framework of the zonal method, considers that a participating medium can be replaced by a few gases (usually, three) with constant absorption coefficient. The absorption coefficient and the weighting factor of each gray gas can be obtained by the fit of the total emitance curve. Smith *et al*. (1982) presented coefficients to carbon dioxide and water vapor mixtures. Recently, Dorigon *et al*. (2013) obtained new WSGG coefficients based on the HITEMP 2010 database (Rothman *et al*., 2010).

Denison and Webb (1993) developed the spectral line weighted-sum-of-gray-gases (SLW) model based in the absorption line blackbody (ALB) distribution function. The integration of the RTE with the SLW model in non-isothermal and non-homogeneous medium produces Leibniz terms, which difficult the RTE solution with standard solvers. As alternative, the model embodies the scaling approximation (Denison and Webb, 1995), which uncouples the spatial and spectral dependences of the absorption cross-section coefficient. This assumption fixes the spectral intervals and, thus, makes the Leibniz terms disappear from the RTE. Whether the spectral intervals remain fixed with the thermodynamic state variation, the ALB distribution function also remains unchanged. This is the reference approach, which is applied to calculate the gray gas absorption coefficient. In the SLW model, the gray gas weighting factor is obtained from the difference between two ALB distribution functions calculated in the supplemental absorption cross-sections.

The cumulative wavenumber (CW) model (Solovjov and Webb, 2002) is also based in a distribution function. In this model, the spectral integration is replaced by the integration of the cumulative distribution function. The integration of the RTE is performed on fixed spectral intervals; therefore it does not produce Leibniz terms. To tackle with non-isothermal and non-homogeneous problems, the CW model uses a local-spectrum correlation. This correlation uncouples the spatial and spectral dependences of the cumulative distribution function. However, the model formulation generally leads to a fail in the energy balance (Galarça *et al*., 2011).

In this work the WSGG model was selected to solve some non-isothermal and non-homogeneous problems. The participating media, a mixture of water vapor and carbon dioxide, is confined between two parallel plates infinitely long. The radiative heat flux and radiative heat source results obtained with WSGG model are compared with the line-by-line integration, while the profiles of temperature and species concentations employed as inputs for the radiative calculations were taken from the literature for a real combustion chamber simulation. The correlations obtained by Dorigon *et al*. (2013) for stoichiometric combustion of methane in air, with water vapor and carbon dioxide partial pressure ratio $p_{\mathrm{H2O}}/p_{\mathrm{CO2}} = 2$, are employed here for situations where $p_{\mathrm{H2O}}/p_{\mathrm{CO2}}$ has an average value greater than 2.0, besides its strongly variation inside the medium, as also is present such a variation in the temperature profiles. These highly non-isothermal and non-homogeneous profiles represent a complex scenario for radiation calculations. The benchmark LBL solutions are conducted with the most recent version of the HITEMP database.

2. THE RADIATIVE TRANSFER EQUATION FOR A PLANE PARALLEL MEDIUM

When the participating medium is comprised by water vapor and carbon dioxide, the scattering effect can be neglected because the molecules are small relative to the wavenumber range of thermal radiation. Therefore, the radiative transfer equation (RTE) is given by:

$$\frac{dI_\eta}{ds} = -\kappa_\eta I_\eta + \kappa_\eta I_{b\eta} \tag{1}$$

where I_η is the spectral radiation intensity along a path *s*, $I_{b\eta}$ is the spectral blackbody radiation intensity and κ_η is the absorption coefficient. The first and the second terms in the right hand side of RTE represent, respectively, attenuation due to absorption and augmentation due to emission. For engineering applications, κ_η is obtained by the Lorentz collision profile (Howell *et al*., 2011),

$$\kappa_\eta = NC_\eta = \sum_i \frac{S_i}{\pi} \frac{\gamma_i}{\gamma_i^2 + (\eta - \eta_i)^2} \tag{2}$$

where *N* is the molar density, C_η is the absorption cross-section coefficient, S_i is the line intensity, γ_i is the line half-width and η_i is the line location. The parameters S_i, γ_i and η_i are obtained from the HITEMP 2010 database (Rothman *et al*., 2010), which is recommended for combustion problems. The summation of Eq. (2) includes only neighboring lines for which the contribution to C_η is significant. All spectral lines within $\Delta\eta$ on either side of the wavenumber of interest η were included. Dorigon *et al*. (2013) recommended $\Delta\eta = 40\ \mathrm{cm}^{-1}$ and $\Delta\eta = 800\ \mathrm{cm}^{-1}$, respectively, for water vapor and carbon dioxide.

Figure 1 depicts a plane parallel medium studied in this paper. In this case, the RTE can be rewritten for the positive and negative directions, respectively, according to:

$$\mu_l \frac{\partial I_{\eta l}^{+}(s)}{\partial s} = -\kappa_\eta I_{\eta l}^{+}(s) + \kappa_\eta I_{b\eta}(s) \tag{3}$$

$$-\mu_l \frac{\partial I_{\eta l}^{-}(s)}{\partial s} = -\kappa_\eta I_{\eta l}^{-}(s) + \kappa_\eta I_{b\eta}(s) \tag{4}$$

where μ_l represents the cosine in the *l* direction, $I_{\eta l}^{+}$ and $I_{\eta l}^{-}$ are the spectral intensities for $\mu_l > 0$ e $\mu_l < 0$, respectively. Considering black walls in the positions *s* = 0 e *s* = *S*, the boundary conditions become, respectively, $I_{\eta l}^{+}(0) = I_{b\eta}(0)$ e $I_{\eta l}^{-}(S) = I_{b\eta}(S)$.

ISSN 2176-5480

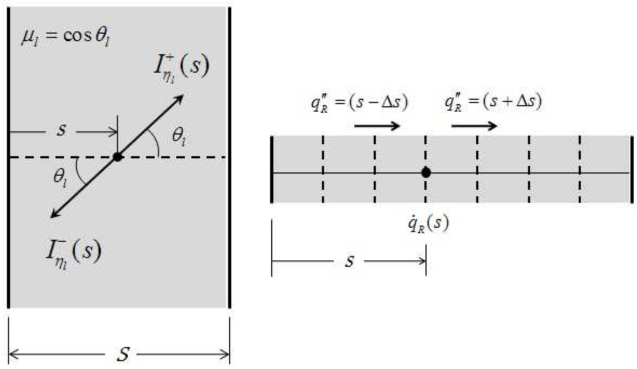

Figure 1. Schematic representation of the one-dimensional domain.

The radiative heat flux q''_R, in W/m², is given by:

$$q''_R(s) = \sum_l \int_\eta 2\pi\mu_l\omega_l \left[I^{+}_{\eta l}(s) - I^{-}_{\eta l}(s)\right] d\eta \tag{5}$$

The radiative heat source $\dot{q}_R$, in W/m³, is given by:

$$\dot{q}_R(s) = \sum_l \int_\eta \left\{2\pi\kappa_\eta\omega_l \left[I^{+}_{\eta l}(s) + I^{-}_{\eta l}(s)\right] - 4\pi\kappa_\eta I_{b\eta}\right\} d\eta \tag{6}$$

where ω_l is the quadrature weight in the direction l. In the previous equations the spectral integration is performed with the LBL method and the integration over the directions is conducted with the Gauss-Legendre quadrature.

When the medium is comprised of a gas mixture, the absorption coefficient required in the previous equations is a summation over all the absorbing species. For a binary mixture of carbon dioxide and water vapor, the absorption coefficient without overlapping effect is:

$$\kappa_\eta = \kappa_{\eta,\mathrm{CO2}} + \kappa_{\eta,\mathrm{H2O}} \tag{7}$$

3. THE WEIGHTED-SUM-OF-GRAY-GASES MODEL

The weighted-sum-of-gray-gases (WSGG) model, first proposed by Hottel and Sarofim (1967), replaces the highly irregular behavior of the absorption coefficient of a real gas by a certain number of gray gases (usually, three) with constant absorption coefficient. Additionally, the transparent windows are induced to ensure the energy balance.

In general, the WSGG parameters can be obtained by the best fit of the total emitance ε. For an isothermal and homogeneous gas, the total emitance of a medium along a path s is given by (Howell *et al*., 2011):

$$\varepsilon(s) = \pi \frac{\int_0^\infty I_{b\eta}\left[1 - e^{-\kappa_{p\eta} ps}\right] d\eta}{\sigma T^4} \tag{8}$$

where $\kappa_{p\eta}$ is the pressure absorption coefficient and, for a gas mixture, p is the sum of the partial pressures of the chemical species, σ is the Stefan-Boltzmann constant and T is the temperature. The product ps is the path-length. For a binary mixture of carbon dioxide and water vapor, the pressure absorption coefficient is obtained by the following relation:

$$\kappa_{p\eta} = \frac{p_{\mathrm{CO2}}\kappa_{p\eta,\mathrm{CO2}} + p_{\mathrm{H2O}}\kappa_{p\eta,\mathrm{H2O}}}{p} \tag{9}$$

After the LBL integration of the Eq. (8), the total emitance ε in the weighted-sum-of-gray-gases (WSGG) model is obtained according to:

ISSN 2176-5480

$$\varepsilon(s)=\sum_{j=0}^{m}a_j(T)\left[1-e^{-\kappa_{p,j}ps}\right] \tag{10}$$

where a_j and $\kappa_{p,j}$ are, respectively, the weighting factor and the pressure absorption coefficient of the *j*-th gray gas. The summation is over *m* gray gases and *j* = 0 represents the transparent windows, with null absorption coefficient. A mathematical interpretation, reveal that a_j and $\kappa_{p,j}$ are the values that give the best fit between Eq. (8) and Eq. (10).

The weighting factor a_j of the *j*-th gray gas has a polynomial dependence on the temperature and is given by:

$$a_j=\sum_{k=1}^{m}b_{j,k}T^{k-1} \tag{11}$$

where $b_{j,k}$ are the polynomial coefficients.

The weighting factor also can be interpreted as a fraction of blackbody energy in the spectrum regions where the gray gas absorption coefficient is $\kappa_{p,j}$. Hence, to ensure the energy balance in the model, the weighting factor for the transparent windows is given by:

$$a_0=1-\sum_{k=1}^{m}a_j \tag{12}$$

As demonstrated by Modest (1991), the WSGG form of the RTE for arbitrary solution method is:

$$\frac{dI_j}{ds}=\kappa_{p,j}p\left(a_jI_b-I_j\right) \tag{13}$$

where I_j is the gray gas intensity and $I_b=\sigma T^4/\pi$.

For stoichiometric combustion of methane in air, the partial pressures of water vapor and carbon dioxide are, respectively, $p_{\mathrm{H2O}}=0.2$ atm and $p_{\mathrm{CO2}}=0.1$ atm. Table 1 presents the coefficients obtained by Dorigon *et al.* (2013) form the HITEMP 2010 database for $p_{\mathrm{H2O}}/p_{\mathrm{CO2}}=2$. The correlations were fitted for path-lengths ranging from 0.001 atm.m to 10 atm.m and for temperature varying between 400 K and 2500 K.

Table 1. WSGG coefficients for H_2O/CO_2 mixtures with $p_{\mathrm{H2O}}/p_{\mathrm{CO2}}=2$,
0.001 atm·m ≤ Ps ≤ 10 atm·m and 400 K ≤ T ≤ 2500 K.

j	$\kappa_{p,j}$ (atm·m)$^{-1}$	$b_{j,1}$	$b_{j,2}$ (K^{-1})	$b_{j,3}$ (K^{-2})	$b_{j,4}$ (K^{-3})	$b_{j,5}$ (K^{-4})
1	0.192	5.617×10^{-2}	7.844×10^{-4}	-8.563×10^{-7}	4.246×10^{-10}	-7.440×10^{-14}
2	1.719	1.426×10^{-1}	1.795×10^{-4}	-1.077×10^{-8}	-6.971×10^{-11}	1.774×10^{-14}
3	11.370	1.362×10^{-1}	2.574×10^{-4}	-3.711×10^{-7}	1.575×10^{-10}	-2.267×10^{-14}
4	111.016	1.222×10^{-1}	-2.327×10^{-5}	-7.492×10^{-8}	4.275×10^{-11}	-6.608×10^{-15}

For a plane parallel medium, the RTE with WSGG model can be rewritten for the positive and negative directions, respectively, according to:

$$\mu_l\frac{\partial I_{jl}^{+}(s)}{\partial s}=-\kappa_{p,j}pI_{jl}^{+}(s)+\kappa_{p,j}pa_jI_b(s) \tag{14}$$

$$-\mu_l\frac{\partial I_{jl}^{-}(s)}{\partial s}=-\kappa_{p,j}pI_{jl}^{-}(s)+\kappa_{p,j}pa_jI_b(s) \tag{15}$$

ISSN 2176-5480

where I_{jl}^{+} e I_{jl}^{-} are the radiation intensities of the *j*-th gray gas to $\mu_l > 0$ e $\mu_l < 0$, respectively. Considering black walls in the positions *s* = 0 e *s* = *S*, the boundary conditions are $I_{jl}^{+}(0) = a_j(0)I_b(0)$ and $I_{jl}^{-}(S) = a_j(S)I_b(S)$.

The radiative heat flux and the radiative heat source are given, respectively, by:

$$q''_R(s) = \sum_l \sum_j 2\pi\mu_l\omega_l \left[I_{jl}^{+}(s) - I_{jl}^{-}(s)\right] \tag{16}$$

$$\dot{q}_R(s) = \sum_l \sum_j \left\{2\pi\kappa_{p,j}\, p\omega_l \left[I_{jl}^{+}(s) + I_{jl}^{-}(s)\right] - 4\pi a_j \kappa_{p,j}\, p I_b(s)\right\} \tag{17}$$

In the previous equations, the WSGG model is used to perform the spectral integration. Therefore, the integration over the wavenumber was replaced by a summation over all gray gases.

The WSGG model was proposed to solve isothermal and homogeneous medium (Hottel and Sarofim, 1967), however, as demonstrated in Dorigon *et al*. (2013) the model solution agrees with the LBL results even in non-isothermal and non-homogeneous conditions.

4. RESULTS

In the present work, the temperature and species concentration profiles were taken from the combustion chamber simulations reported by Centeno *et al*. (2013) where it was considered non-premixed turbulent combustion of methane-air. Natural gas is injected into the chamber by a duct aligned with the chamber centerline, leading to a non-swirling flame, while air enters the chamber through a centered annular duct. The burner provides the necessary amount of air and natural gas as required by the process, with a prescribed fuel excess of 5 %. The Reynolds number at the entrance, approximately 1.8×10^4, points that the flow is turbulent. The burner power is about 600 kW. Figure 2 depicts some sections in the combustion chamber for which the temperature and species concentration profiles were obtained. The radial sections 1, 2 e 3 are placed, respectively, at 0.312 m, 0.912 m and 1.312 m from the chamber entrance. The section 4 overlaps to the chamber center line. The problem is solved as an one-dimensional medium bounded by black walls at *T* = 393.15 K. The total pressure is 1 atm. The dimensionless radius and length are given by $r^* = r/R$ and $x^* = x/L$, respectively.

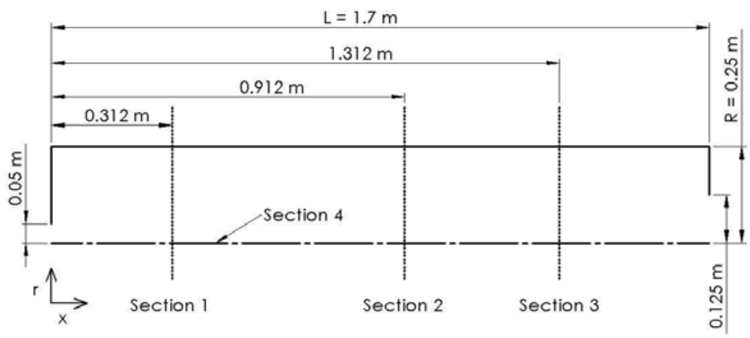

Figure 2. Combustion chamber geometry (Centeno *et al*., 2013).

The results are displayed in terms of the radiative heat flux and the radiative heat source. The local errors in q''_R and $\dot{q}_R$ are calculated, respectively, as:

$$\delta[\%] = 100\frac{\left|q''_{R,\mathrm{WSGG}} - q''_{R,\mathrm{LBL}}\right|}{\max\left|q''_{R,\mathrm{LBL}}\right|} \tag{18}$$

$$\xi[\%] = 100 \frac{\left|\dot{q}_{R,\mathrm{WSGG}} - \dot{q}_{R,\mathrm{LBL}}\right|}{\max\left|\dot{q}_{R,\mathrm{LBL}}\right|} \tag{19}$$

where $\max\left|q''_{R,\mathrm{LBL}}\right|$ and $\max\left|\dot{q}_{R,\mathrm{LBL}}\right|$ are the maximum absolute values of the radiative heat flux and the radiative heat source in the LBL solution for each studied case. The quantity $\dot{q}_R$ represents a balance between the energy absorbed and emitted by a participating medium. Furthermore, in combined heat transfer problems, $\dot{q}_R$ is the source term in the equation of energy.

Figures 3-6 depict the temperature and species concentration profiles for the sections showed in Fig. 2. In all cases, the average partial pressure ratio $(p_{\mathrm{H2O}} / p_{\mathrm{CO2}})_{\mathrm{avg}}$ is greater than 2.0 and presents strong variation with the position, as also observed for the temperature and species concentration profiles. In Figure 3(a), the temperature is 326.64 K at the centerline ($r^* = 0$) and the maximum temperature is 1057.90 K. The temperature at the centerline is 539.40 K and the maximum temperature is 1384.70 K to the Fig. 4(a). In the Figure 5(a), the temperature is 1462.70 K at the centerline and the maximum value is 1561.40 K. In the axial section, Figure 6(a), the temperature is 313.15 K at the chamber entrance ($x^* = 0$) and the maximum temperature is 1636.30 K

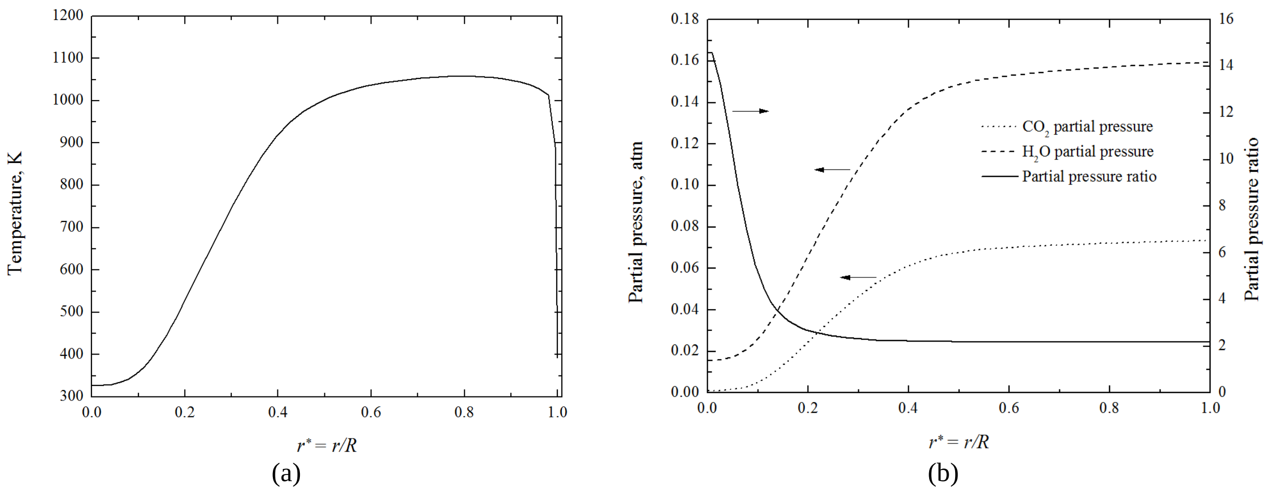

Figure 3. Section 1: (a) temperature, (b) partial pressure – $(p_{\mathrm{H2O}} / p_{\mathrm{CO2}})_{\mathrm{avg}}$ = 3.53.

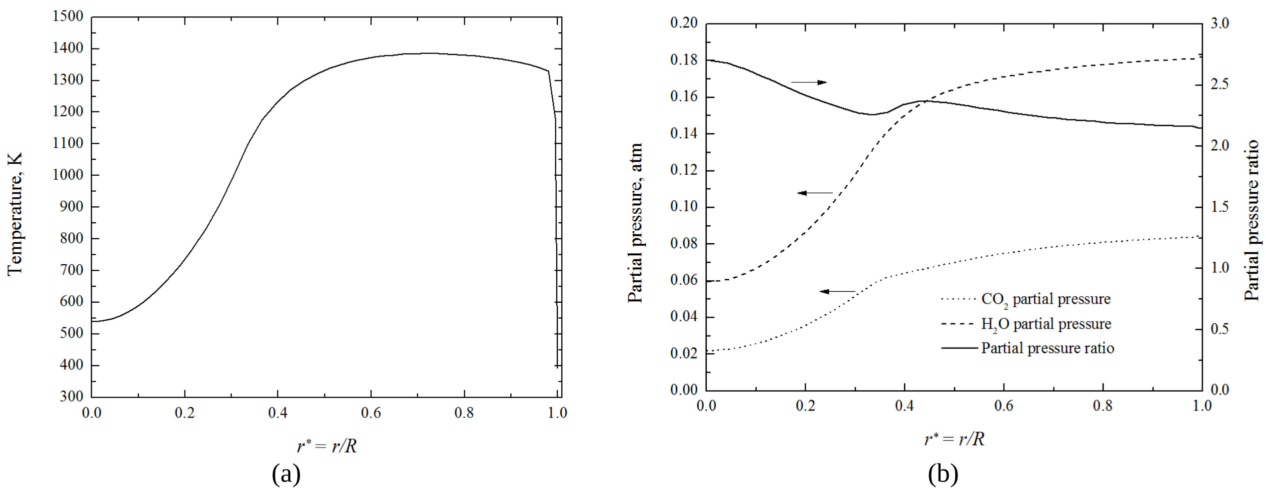

Figure 4. Section 2: (a) temperature, (b) partial pressure – $(p_{\mathrm{H2O}} / p_{\mathrm{CO2}})_{\mathrm{avg}}$ = 2.35.

ISSN 2176-5480

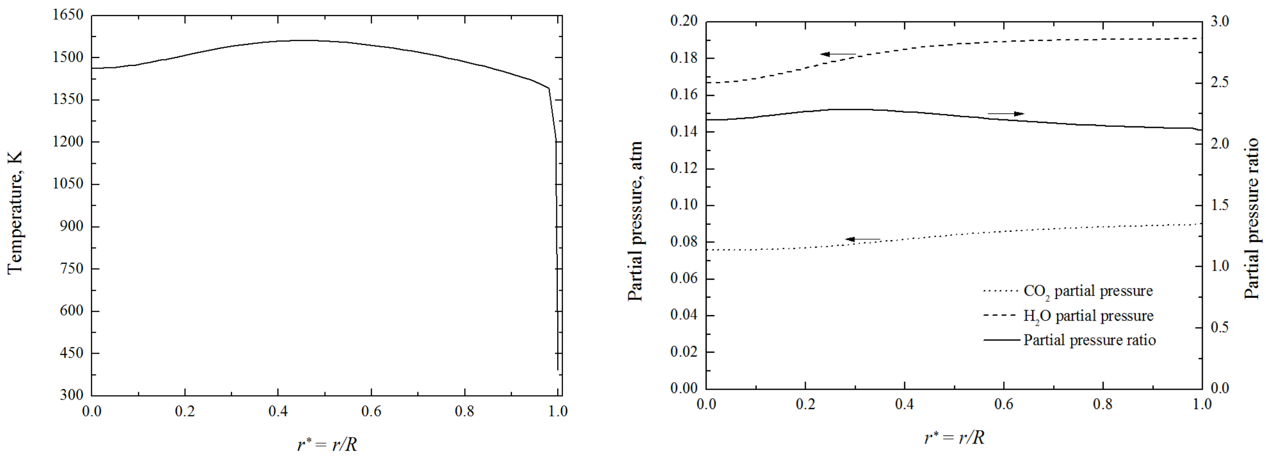

(a) (b)

Figure 5. Section 3: (a) temperature, (b) partial pressure – $\left(p_{H2O}/p_{CO2}\right)_{avg}$ = 2.21.

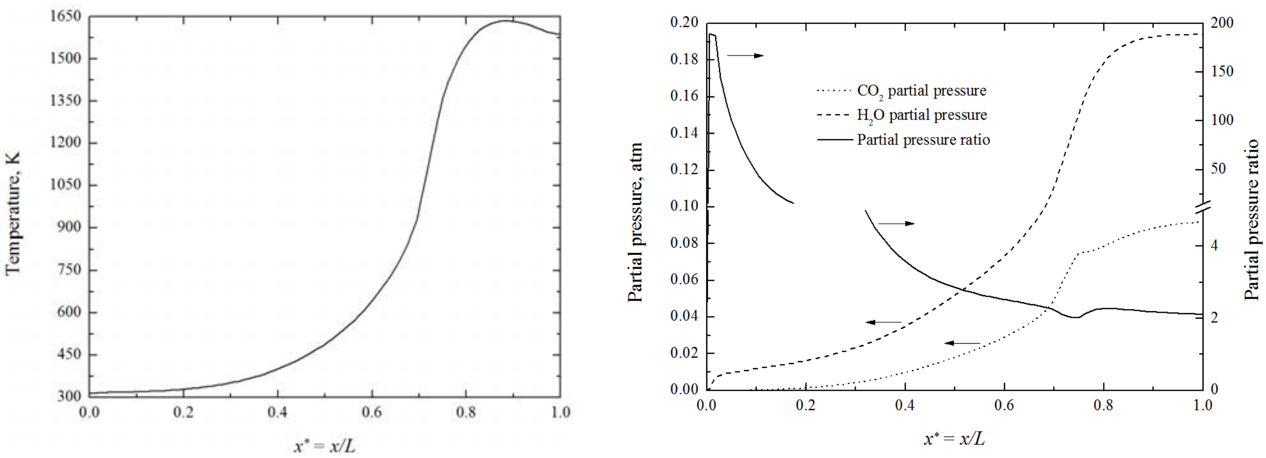

(a) (b)

Figure 6. Section 4: (a) temperature, (b) partial pressure – $\left(p_{H2O}/p_{CO2}\right)_{avg}$ = 16.13.

Figures 7(a) and 7(b) present the radiative heat flux and the radiative heat source for the section 1, located at 0.312 m from the chamber entrance. The temperature and partial pressure profiles are showed, respectively, in the Fig. 3(a) and 3(b). For the radiative heat flux, as depicted in the Table 2, the maximum and average errors are 9.2 % and 6.2 %, respectively. As showed in Tab. 3, for the radiative heat source, the maximum error is 52.5 %, however the average error is 2.0 %. As depicted in the Fig. 8 the maximum error in $\dot{q}_R$ is attained close to the wall, where the temperature changes sharply (as observed in Fig. 3(a)). Despite the strong variation in the partial pressure ratio close to the center line, there are overall good agreement between WSGG and LBL solutions, since the temperature is low in the portion of Section 1 next to the center line.

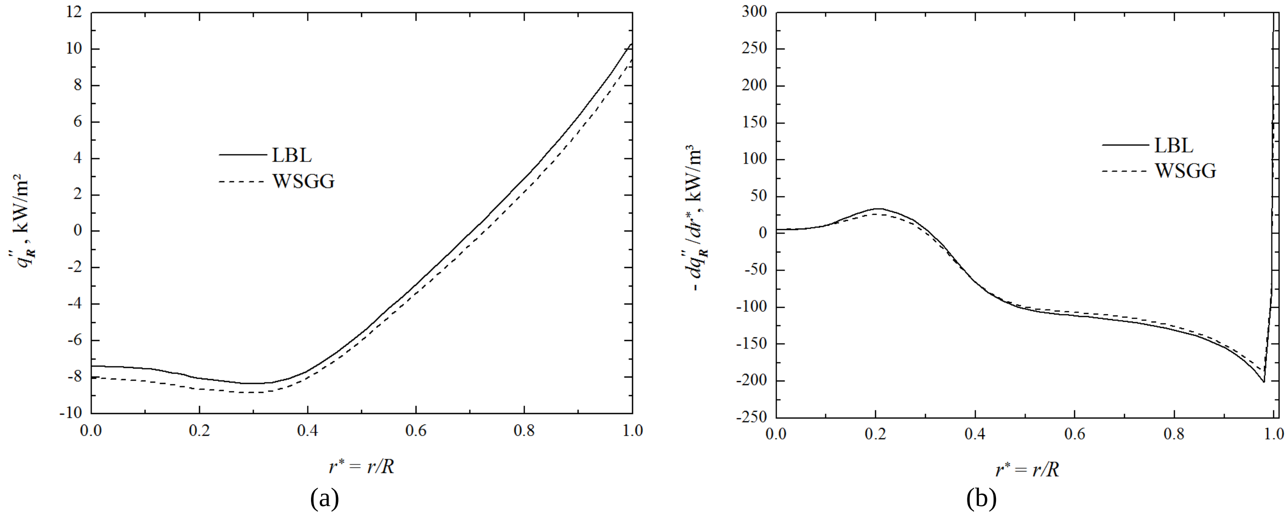

Figure 7. Results for section 1: (a) Radiative heat flux, (b) radiative heat source $\left(\dot{q}_R = -dq''_R / dr^*\right)$.

Section 2 is located at 0.912 m from the chamber entrance. In this case, the temperature and partial pressure profiles are showed, respectively, in Figs. 4(a) and 4(b). Figure 9(a) presents the radiative heat flux. As depicted in the Table 2, the maximum and average errors in the radiative heat flux are, respectively, 3.9 % and 1.8 %. The average partial pressure ratio was increased in relation to the previous section, but the errors in the heat flux calculation were decreased. In the radiative heat source, the maximum and average errors are 56.0 % and 2.2 %, respectively, as showed in Tab. 3. As showed in the Fig. 10, again the maximum error occurs only in the vicinity of the wall because the strong variation in the temperature.

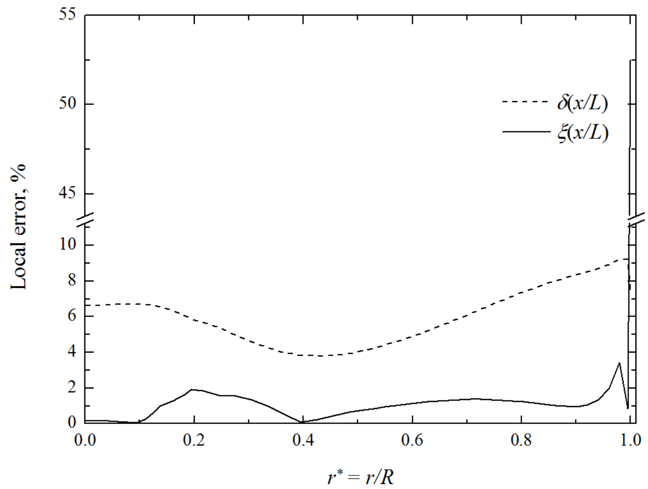

Figure 8. Local error along the section 1.

ISSN 2176-5480

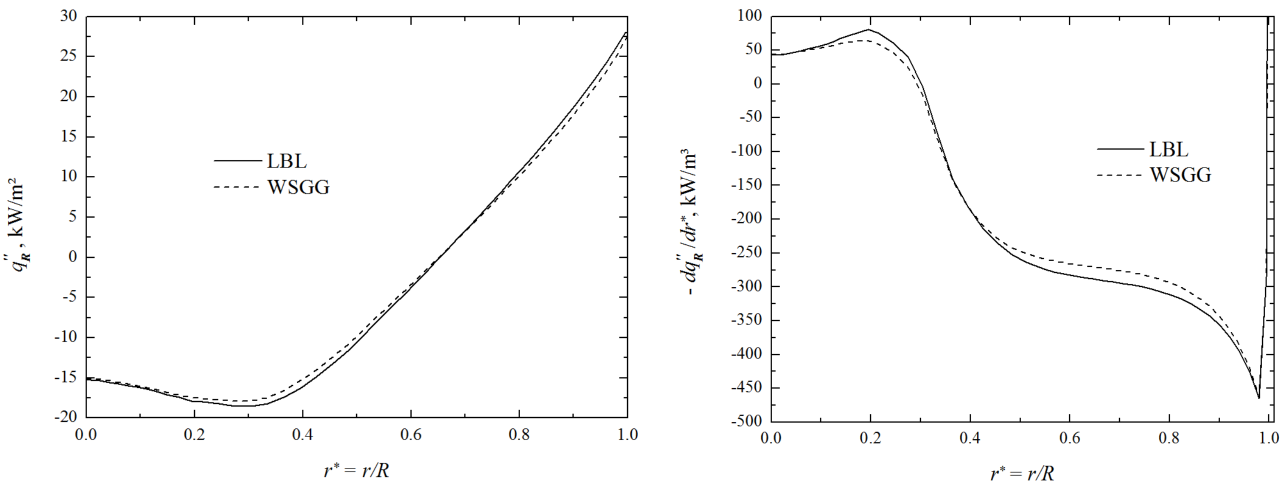

(a) (b)

Figure 9. Results for section 2: (a) Radiative heat flux, (b) radiative heat source $\left(\dot{q}_R = -dq''_R / dr^*\right)$.

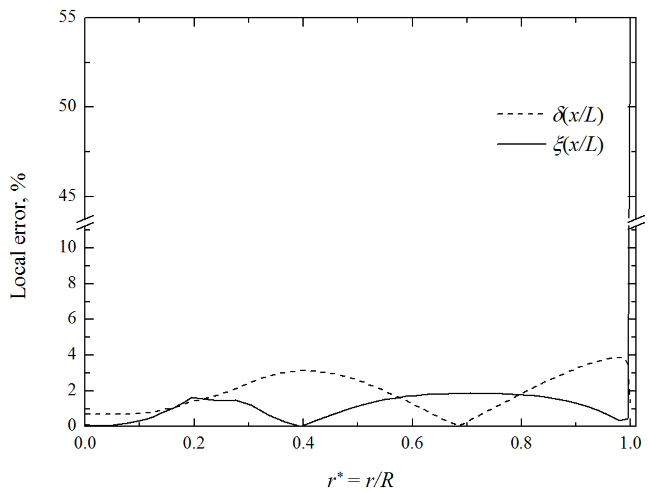

Figure 10. Local error along the section 2.

For Section 3, positioned at 1.312 m from the chamber entrance, the temperature and partial pressure profiles are showed, respectively, in the Fig. 5(a) and 5(b). Figures 11(a) and 11(b) present the radiative heat flux and the radiative heat source. As depicted in the Table 2, the maximum and average errors in the radiative heat flux are, respectively, 1.9 % and 1.6 %. In the radiative heat source, the maximum and average errors are 57.4 % and 1.6 %, respectively, as showed in Tab. 3. As in the previous cases, due to the strong change in the temperature, the maximum error in the radiative heat source only happens close to the wall. The reduction in the averages errors can be attributed to the slightly variation in the partial pressure ratio. The reduction in the average errors also can be credited to the temperature profile, Fig. 5(a), which is almost an isothermal problem.

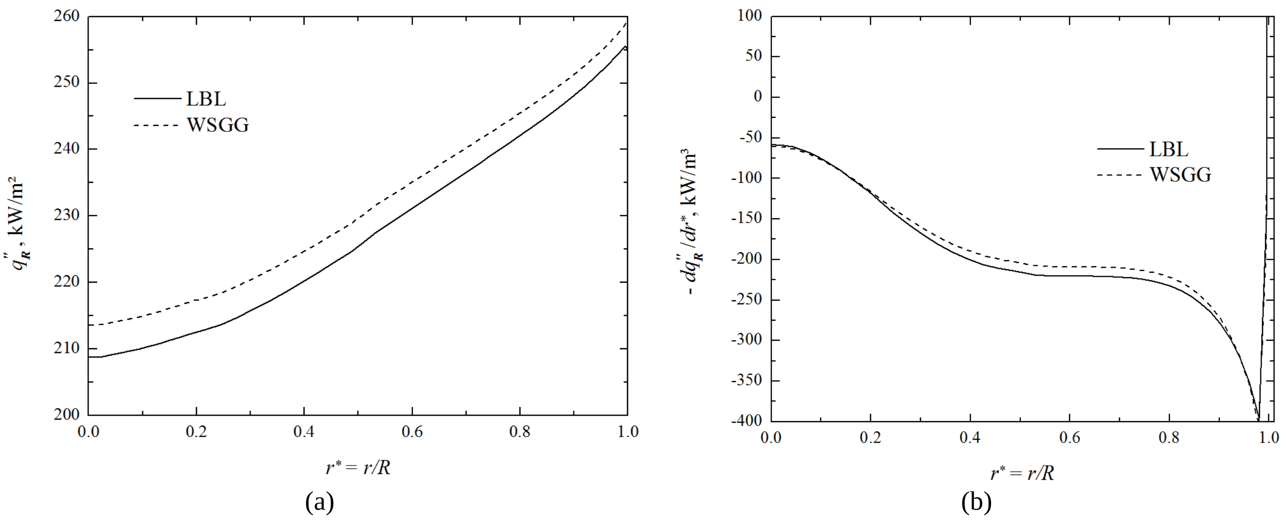

Figure 11. Results for section 3: (a) Radiative heat flux, (b) radiative heat source $\left(\dot{q}_R = -dq''_R / dr^*\right)$.

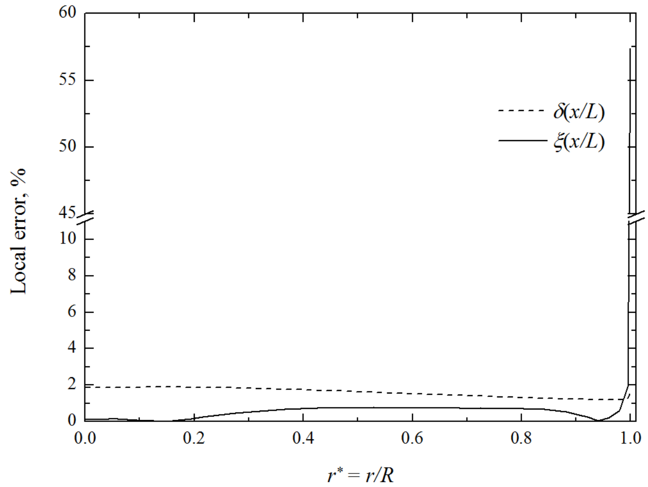

Figure 12. Local error along the section 3.

Figures 13(a) and 13(b) present the radiative heat flux and the radiative heat source for Section 4, placed along the chamber axis. The temperature and partial pressure profiles are showed, respectively, in the Fig. 6(a) and 6(b). As depicted in the Table 2, the maximum and average errors in the radiative heat flux are, respectively, 3.4 % and 3.2 %. In the radiative heat source, the maximum and average errors are 7.4 % and 1.4 %, respectively, as showed in Tab. 3. In this last case, the optical thickness was increased. This can explain why the radiative heat source was reduced when compared with the previous sections. In spite the strong variation in the partial pressure ratio close to the chamber entrance, observed in the Fig. 6(b), the WSGG solution agrees adequately with the LBL solution because the temperature along the axial direction and next to the beginning of the chamber is very low.

ISSN 2176-5480

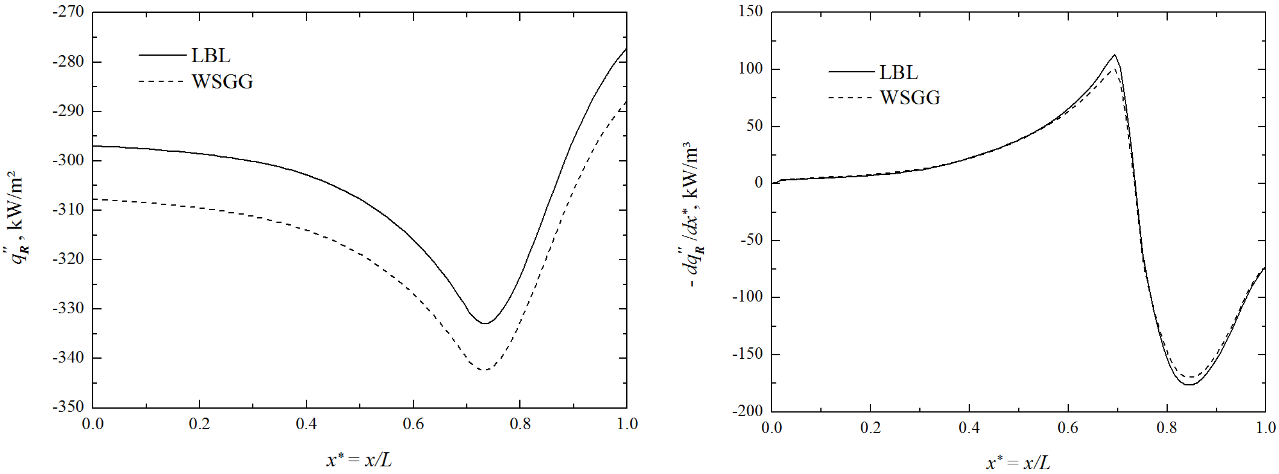

(a) (b)

Figure 13. Results for section 4: (a) Radiative heat flux, (b) radiative heat source $\left(\dot{q}_R = -dq''_R / dx^*\right)$.

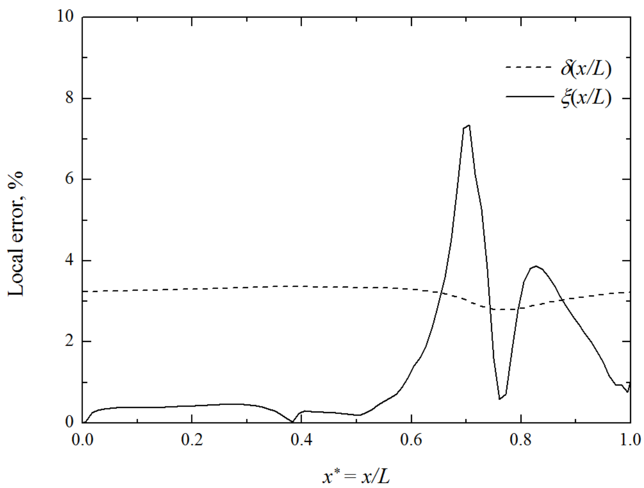

Figure 14. Local error along the section 4.

Table 2. Maximum $\delta_{\max}$ and average δ_{avg} errors in the WSGG solution for the radiative heat flux.

Section	$(p_{H2O}/p_{CO2})_{avg}$	$\delta_{\max}$ (%)	δ_{avg} (%)
1	3.53	9.2	6.2
2	2.35	3.9	1.8
3	2.21	1.9	1.6
4	16.13	3.4	3.2

Table 3. Maximum $\xi_{\max}$ and average ξ_{avg} errors in the WSGG solution for the radiative heat source.

Section	$(p_{H2O}/p_{CO2})_{avg}$	$\xi_{\max}$ (%)	ξ_{avg} (%)
1	3.53	52.5	2.0
2	2.35	56.0	2.2
3	2.21	57.4	1.6
4	16.13	7.4	1.4

5. CONCLUSIONS

This work presented the solution of the radiation heat transfer in some non-isothermal and non-homogeneous medium comprised by carbon dioxide and water vapor. The temperature and species partial pressure profiles were obtained from a combustion chamber and the problem was solved as an one-dimensional medium. The spectral integration of radiative transfer equation was performed with the line-by-line (LBL) method and the weighted-sum-of-gray-gases (WSGG) model. The WSGG correlations applied in this work were proposed to stoichiometric combustion of methane, with constant partial pressure ratio. However the results showed good overall agreement between WSGG and LBL solutions, even with high variation in the average partial pressure ratio. The average errors were less than 7.0 %. In some cases, the maximum error in the radiative heat source can be attributed to the strong variation in the temperature close to the walls. This paper showed that the WSGG model is a good alternative to the LBL computationally expensive calculations in combustion problems.

6. ACKNOWLEDGEMENTS

FC and RB thank CNPq due to its financial support by means of a Doctoral Degree scholarship.

7. REFERENCES

Centeno, F.R., França, F.H.R., Cassol, F. and da Silva, C.V., 2013. “Comparison of different WSGG correlations in the computation of thermal radiation in a 2D axisymmetric turbulent non-premixed methane-air flame”. *Journal of the Brazilian Society of Mechanical Sciences and Engineering*, Vol. 35, p. 419-430.

Denison, M.K. and Webb, B.W., 1993. “A spectral line-based weighted-sum-of-gray-gases model for arbitrary RTE solvers”. *Journal of Heat Transfer*, Vol. 115, p. 1004-1012.

Denison, M.K. and Webb, B.W., 1995. “The spectral line-based weighted-sum-of-gray-gases model in nonisothermal nonhomogeneous media”. *Journal of Heat Transfer*, Vol. 117, p. 359-365.

Dorigon, L.J., Duciak, G., Brittes, R., Cassol, F., Galarça, M. and França, F.H.R., 2013. “WSGG correlations based on HITEMP2010 for computation of thermal radiation in non-isothermal, non-homogeneous H_2O/CO_2 mixtures”. *International Journal of Heat and Mass Transfer*, Vol. 64, p. 863-873.

Galarça, M.M., Mossi, A. and França, F.H.R., 2011. “A modification of the cumulative wavenumber method to compute the radiative heat flux in non-uniform media”. *Journal of Quantitative Spectroscopy & Radiative Transfer*, Vol. 112, p. 384-393.

Hottel, H.C. and Sarofim, A.F., 1967. *Radiative Transfer*. McGraw-Hill, New York.

Howell, J.R, Siegel, R., and Mengüç, M.P., 2011. *Thermal Radiation Heat Transfer*. Taylor & Francis, New York, 5th edition.

Modest, M.F., 1991. “The weighted-sum-of-gray-gases model for arbitrary solution methods in radiative transfer”. *Journal of Heat Transfer*, Vol. 113, p. 650-656.

Rothman, L.S., Gordon I.E., Barber, R.J., Dothe, H., Gamache, R.R., Goldman, A., Perevalov, V.I., Tashkun, S.A. and Tennyson, J., 2010. “HITEMP, the high-temperature molecular spectroscopy database”. *Journal of Quantitative Spectroscopy & Radiative Transfer*,Vol. 111, p. 2139-2150.

Smith, T.F., Shen, Z.F. and Friedman, J.N., 1982. “Evaluation of coefficients for the weighted sum of gray gases model”. *Journal of Heat Transfer*, Vol. 104, p. 602-608.

Solovjov, V.P. and Webb, B.W., 2002. “A local-spectrum correlated model for radiative transfer in non-uniform gas media”. *Journal of Quantitative Spectroscopy & Radiative Transfer*, Vol. 73, p. 361-373.

8. RESPONSIBILITY NOTICE

The authors are the only responsible for the printed material included in this paper.